

---

# PuzzleFusion: Unleashing the Power of Diffusion Models for Spatial Puzzle Solving [Supplementary Material ]

---

Anonymous Author(s)

Affiliation

Address

email

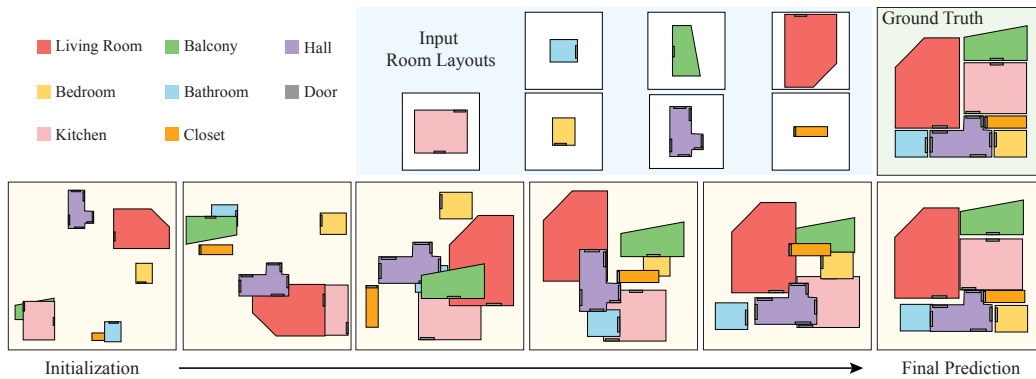


Figure 1: Room layout arrangement is the task of taking a set of room layouts and their corresponding room types as the input and predicting the position and the orientation of each room. The biggest discovery and surprise of this paper is that conditional generation by a Diffusion Model solves this challenging problem.

1 The supplementary document provides more details on our system and the competing methods  
2 (Sect. A), more details on the datasets (Sect. B), additional ablation studies (Sect. C), and additional  
3 qualitative examples (Figs. 2, and 4, 3, 8, 9) as promised in the main paper. Figure 2 visualizes the  
4 samples predicted by our method at step  $t$ . Figure 4 shows more qualitative evaluations of our method  
5 for Full MagicPlan and Full RPLAN datasets. Figure 3 shows more qualitative evaluations of our  
6 approach against the three competing methods. Please also see the supplementary video for more  
7 examples.

## 8 A Methods details of our system and competing methods

9 We benefit from Transformers in our task in two ways. First, Transformers provide the capability  
10 of processing sequences with different lengths, which we use to process different number of room  
11 layouts/corners in the houses. Second, we utilize the self-attention module of Transformers to  
12 create optimal interaction and information-sharing among input tokens. These two features make  
13 Transformers an ideal backbone for our model. Our method uses six Transformer encoder blocks,  
14 and attention in each block has four heads. We also use an MLP For converting 256D Transformer  
15 output to rotation and position (4D). To keep the experiments fair, we use the same architecture for  
16 our transformer baselines as much as possible. In the following, we provide details corresponding to  
17 each of the baselines.

18 **Transformer with a raster representation** (TransRaster) uses the raster images to represent the  
19 input room layouts/types and the output room positions. Note that this baseline does not handle  
20 rotations as explained below. An input room layout is represented as a 20-channel  $256 \times 256$  semantic  
21 segmentation image, where there are 20 room/door types. The room center is aligned with the center  
22 of an image. An output room position is represented as a  $256 \times 256$  room occupancy image, which  
23 is ideally a translated version of the input room segmentation image at the correct room location.  
24 Given an output room occupancy image, we perform an exhaustive search over the possible room  
25 translations and find one with the most overlap between the occupancy image and the translated room  
26 segmentation image.<sup>1</sup> We use VisionTransformer [1] with a CNN decoder that takes a set of input  
27 room segmentation images and produces a set of room occupancy images.

28 In the other word TransRaster uses an encoder part of U-Net, which has 8 down-sampling blocks,  
29 converting each input room layout to a feature map of dimension 512. Each feature map (correspond-  
30 ing to a room layout) will become one input token for the Transformer. Input sequence’s length is  
31 equal to the number of rooms in a house, and information is shared among different rooms. We use  
32 six Transformer encoder blocks, and attention in each block has four heads. We pass the output of  
33 Transformer to a U-Net up-sampling model with eight Up-sampling blocks to change the dimension  
34 from 512 to  $256 \times 256$ .

35 **Transformer with a vector representation** uses the same backbone as our method; a linear layer  
36 converts the 28D input vector (i.e., 2 for the original corner coordinate and 20 for the room/door type  
37 one-hot vector) to the 256D feature map, six Transformer encoder blocks, and the attention in each  
38 block have four heads. We also use an MLP to convert 256D output embedding to 4D output.

39 **Diffusion model, one room per node** encodes each node as corresponding to a room instead of a  
40 corner in the room. To ease the implementation, we set the maximum number of nodes per room to  
41 20 and we pad extra nodes when the room has less than 20 nodes with 0. We flatten the conditions  
42 per room and then use a linear layer to convert it to a 256D embedding vector. Each feature map  
43 represents a room and an input token for Transformer, we use the same Transformer as our method.  
44 After the Transformer blocks, a linear layer converts 256D output to 4D (i.e., 2 for the position and 2  
45 for the rotation).

46 **Shabani et al.** [2] takes the input layout of each room with the resolution of  $256 \times 256$  with the  
47 same number of channels as the number of room types to pass each pixel as a one-hot vector of the  
48 corresponding room type. We use the same model as [2] and change the number of input channels to  
49 11 for RPLAN and 20 for MagicPlan. To generate the arrangement candidates, we use the given room  
50 layouts of our dataset to connect doors, while we also use overlap filtering to reduce the number of  
51 candidates. Note that our datasets is significantly larger than the one in [2], enabling us to randomly  
52 select a positive or a negative candidate in each iteration and therefore remove the class imbalance  
53 weight used in [2]. During the training for each house, we randomly select a GT with the label 1 or a  
54 faulty candidate with the label [0, 1) based on the number of mismatched doors. During the test, we  
55 pass all the possible candidates of each house and select the candidate with the highest score as the  
56 final prediction.

57 **Harel et al.** [3] proposed a two-step algorithm for CJP. Their method considers two types of constraints  
58 to find plausible mates based on the length and angle of different pairs of connections. By estimating  
59 the matings hierarchically using these constraints, they approach the problem of finding positions as  
60 a multi-body spring-mass system. We utilize the authors’ provided implementation<sup>2</sup> for comparison  
61 with our method. With a test dataset of 1000 crossing-cut puzzles, we restrict the running time of the  
62 spring-system algorithm to 2 minutes per puzzle. Furthermore, unlike the provided implementation,  
63 we also consider failure cases in the metrics. Regarding the pictorial case, the authors score a  
64 candidate mating by extrapolating the images of puzzle pieces and considering the difference of the  
65 mean color value on the edges. We do not impose any time limit as we evaluate only on 20 samples.

Room Type	3	4	5	6	7	8	9	10	All
Master bedroom	0.20	0.26	0.29	0.32	0.39	0.49	0.49	0.53	0.34
Living room	0.52	0.56	0.59	0.65	0.71	0.75	0.79	0.79	0.65
Kitchen	0.42	0.47	0.52	0.59	0.68	0.71	0.76	0.79	0.59
Bathroom	0.54	0.70	0.85	0.96	1.12	1.28	1.33	1.47	0.96
Toilet	0.07	0.11	0.15	0.22	0.22	0.25	0.27	0.26	0.18
Corridor	0.07	0.12	0.15	0.19	0.25	0.32	0.37	0.45	0.21
Closet	0.13	0.18	0.22	0.32	0.48	0.68	0.92	1.22	0.41
Hall	0.35	0.55	0.68	0.77	0.85	0.91	0.98	1.08	0.73
Laundry room	0.05	0.05	0.05	0.07	0.10	0.13	0.18	0.23	0.09
Bedroom	0.34	0.69	1.08	1.32	1.51	1.74	1.93	2.10	1.23
Balcony	0.05	0.08	0.16	0.32	0.40	0.48	0.56	0.64	0.29
Dining room	0.13	0.12	0.12	0.14	0.17	0.19	0.22	0.25	0.15
Private office	0.00	0.01	0.02	0.05	0.05	0.07	0.08	0.10	0.05
Den	0.05	0.05	0.06	0.7	0.09	0.11	0.12	0.12	0.08
Storage	0.00	0.01	0.01	0.02	0.02	0.02	0.03	0.03	0.02
Others	0.00	0.01	0.01	0.02	0.03	0.04	0.04	0.07	0.03
Doors	2.84	3.82	4.82	5.43	6.92	8.02	6.10	10.18	5.90

Table 1: MagicPlan dataset consists of floorplans with 3 to 10 rooms. The table shows average number of rooms with a specific room type based on the total number of rooms in the house.

## 66 B Datasets Details and Preprocessing

67 We normalize the puzzles/floorplans for each task and dataset by scaling them to fit within a  $1 \times 1$   
68 square, and we also resize all corresponding images to dimensions of  $256 \times 256$  in the case of pictorial  
69 CJP. While this normalization process does not introduce any essential additional information during  
70 testing in CJP and VJP, it could potentially enables the network to cheat in RLA, as the longer extent  
71 of arranged floorplans is always fixed to 1. To address this issue, during testing in RLA, we apply a  
72 random scaling factor in the range of  $[0.8, 1.0]$  to the room shapes of each house. In the subsequent  
73 sections, we provide a detailed description of each dataset. In the following, we provide additional  
74 statistics for our floorplan datasets.

75 The Voronoi Jigsaw Puzzle dataset consists of 200k training puzzles and 1k testing puzzles. These  
76 puzzles were created by randomly selecting 3 to 15 points, The individual pieces of the puzzles were  
77 obtained by extracting the Voronoi cells corresponding to these points. There are 1,066, 14,033,  
78 23,715, 20,279, 16,073, 15,235, 16,428, 15,018, 16,318, 15,096, 16,487, 16,233, and 15,670 puzzles  
79 with 3, 4, 5, 6, 7, 8, 9, 10, 11, 12, 13, 14, and 15 pieces respectively. Each piece has a minimum,  
80 maximum, and average of 3, 20, and 4.51 corners respectively. The minimum, maximum, and average  
81 number of corners per puzzle are 10, 93, and 42.24.

82 Cross-cut Jigsaw Puzzle (CJP) are consist of 100k training and 1k testing puzzles, where each one  
83 were generated using [3] method which generate a convex polygon and cuts it by 3 to 5 lines. There  
84 are 1719, 6046, 15854, 14521, 6905, 10929, 12065, 8361, 6521, 8192, 7663, 4642, 1508, 73, and  
85 1 puzzles with 3, to 18 pieces respectively. Each piece has a minimum, maximum, and average of  
86 3, 13, and 4.47 corners respectively. The minimum, maximum, and average number of corners per  
87 puzzle are 16, 76, and 41.99.

88 MagicPlan dataset consists of roughly 98K houses/apartments, which we divide into 93K training  
89 and 5K testing samples. The number of rooms in a house ranges from 3 to 10. Concretely, 11661,  
90 16322, 19171, 17582, 13200, 9649, 6780, and 4415 houses contain 3, 4, 5, 6, 7, 8, 9, and 10 rooms,  
91 respectively. The minimum and maximum numbers of corners in a house are 12 and 182. Table 1  
92 shows average number of rooms with a specific room type based on the total number of rooms in the  
93 house.

<sup>1</sup>We could expand the search space with possible room rotations, but rooms are often symmetric. To be simple, we use this baseline only for experiments when ground-truth rotations are given.

<sup>2</sup><https://icvl.cs.bgu.ac.il/polygonal-puzzle-solving/>

94 In the RPLAN dataset, we divide 60K samples in RPLAN to 55K train and 5K test. The number of  
 95 rooms in a house ranges from 3 to 8. Concretely 99, 582, 5083, 19551, 21921, and 13235 houses  
 96 contain 3, 4, 5, 6, 7, and 8 rooms, respectively.

## 97 C Additional ablation studies

### 98 C.1 Additional ablation studies on room layout arrangement

Table 2: Main quantitative results with two metrics: Positional Error (MPE) and Graph Editing Distance (GED). This table show a case where the ground-truth rotations are given, as TransRaster baseline cannot handle rotations. Small RPLAN (resp. Small MagicPlan) is a subset of the corresponding full dataset, consisting of houses with at most 6 rooms. The small datasets are created for Shabani *et al.*, which is not scalable to many rooms. Our method is stochastic and shows both the mean and the standard deviation.

Dataset	Small RPLAN		Full RPLAN		Small MagicPlan		Full JigsawPlan	
Metric	MPE ( $\downarrow$ )	GED ( $\downarrow$ )	MPE ( $\downarrow$ )	GED ( $\downarrow$ )	MPE ( $\downarrow$ )	GED ( $\downarrow$ )	MPE ( $\downarrow$ )	GED ( $\downarrow$ )
Shabani <i>et al.</i>	17.6	1.0	$\times$	$\times$	32.2	1.1	$\times$	$\times$
TransRaster	13.9	1.2	15.7	2.1	36.1	2.1	41.9	4.1
TransVector	12.9	1.1	13.9	2.0	37.7	1.9	42.8	4.0
Ours	<b>4.6<math>\pm</math>0.7</b>	<b>0.4<math>\pm</math>0.0</b>	<b>5.4<math>\pm</math>0.7</b>	<b>0.6<math>\pm</math>0.0</b>	<b>17.5<math>\pm</math>0.8</b>	<b>1.0<math>\pm</math>0.4</b>	<b>27.9<math>\pm</math>0.7</b>	<b>2.7<math>\pm</math>0.5</b>

99 Figure 6 shows the raw estimated position information at each room/door corner before the room-wise  
 100 averaging. Since the ground-truth has the same pose parameters for all corners in a room/door, the  
 101 network learns to produce consistent parameters. Figure 7 shows five pose estimation results by  
 102 our system while varying the initial noise  $x_T$ . While there are minor differences, the overall room  
 103 arrangements are similar and close to the ground-truth, indicating that the Diffusion model is capable  
 104 of producing consistent results given enough constraints as a pose estimation system, as opposed to a  
 105 generative model whose original goal is to create a diverse set of answers.

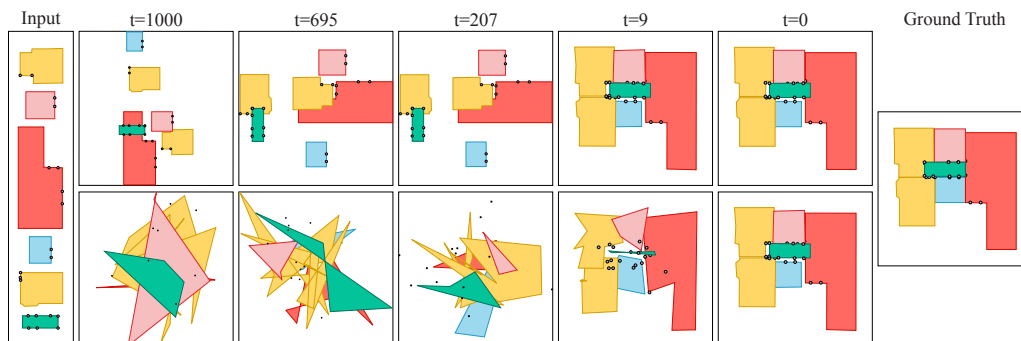


Figure 2: Visualization of predicted layouts at step “t”s. At t=1000, position parameters at each corner are initialized by a Gaussian noise, and at t=0, there is the final predicted layout. The top row shows the predicted layout without averaging/voting, and the bottom row shows with averaging/voting. To make it more clear, we show doors by their corners.

#### 106 C.1.1 Additional ablation on RPLAN

107 The main paper shows the ablation studies on the MagicPlan dataset in case of room layout arrangement  
 108 task. This part of supplementary will present the same study results on RPLAN dataset. Table 3  
 109 shows the impact of our attention module and door matching loss on performance and Table 4 shows  
 110 the impact of noise in the room type and door detection on our performance, although there is a  
 111 performance drop, our method still works better than the competing methods.

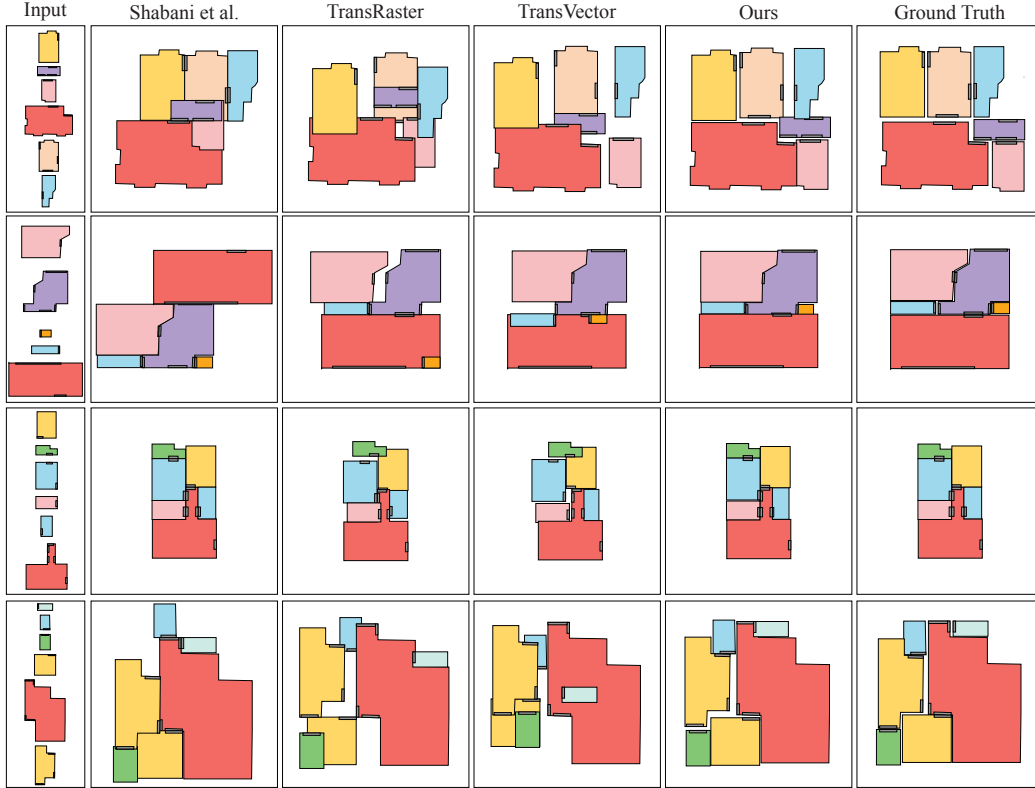


Figure 3: Qualitative evaluations of our approach against the three competing methods. The top two rows are from Small MagicPlan. The bottom two rows is from Small RPLAN. The GT rotations are given for all the cases to enable comparisons with all the methods.

Table 3: Co attention mechanisms (P-SA, G-SA) and the door matching loss ( $L_{match}$ ). Full RPLAN is used.  $\checkmark$  indicates the feature being used. In case of  $L_{match}$  “Doors” means matching loss has been applied only on door corners and “All corners” means matching loss has been applied to all corners including door corners.

P-SA	G-SA	$L_{match}$	MPE ( $\downarrow$ )	GED ( $\downarrow$ )
	$\checkmark$		25.6	1.6
$\checkmark$	$\checkmark$		24.2	1.5
$\checkmark$		Doors	36.9	2.4
	$\checkmark$	Doors	22.1	1.1
$\checkmark$	$\checkmark$	All Corners	10.7	0.9
$\checkmark$	$\checkmark$	Doors	10.5	0.9

Table 4: Effects of the room-type (R-type) and the Door information. Full RPLAN is used.  $\checkmark$  indicates the information being used. When a room-type is not used, we set a zero vector as a room-type one-hot vector. When the door information is not used, we do not pass the door-corner nodes to the network.

Train		Test		MPE( $\downarrow$ )	GED ( $\downarrow$ )
R-Type	Door	R-Type	Door		
$\checkmark$	$\checkmark$		$\checkmark$	17.3	1.4
	$\checkmark$		$\checkmark$	16.4	1.5
$\checkmark$	$\checkmark$	$\checkmark$		15.1	1.9
$\checkmark$		$\checkmark$		14.3	1.9
$\checkmark$	$\checkmark$	$\checkmark$	$\checkmark$	10.5	0.9

## 112 C.2 Additional ablation studies on puzzle solving

113 We have provided additional qualitative results of our method in Figure 8 and Figure 9 including noisy  
 114 samples or samples with missing or duplicate pieces. In case of missing and duplicate experiment,  
 115 we repeat (remove) each piece with a probability of 10%. Table 5 presents the evaluation metrics of  
 116 missing and duplicate experiments.

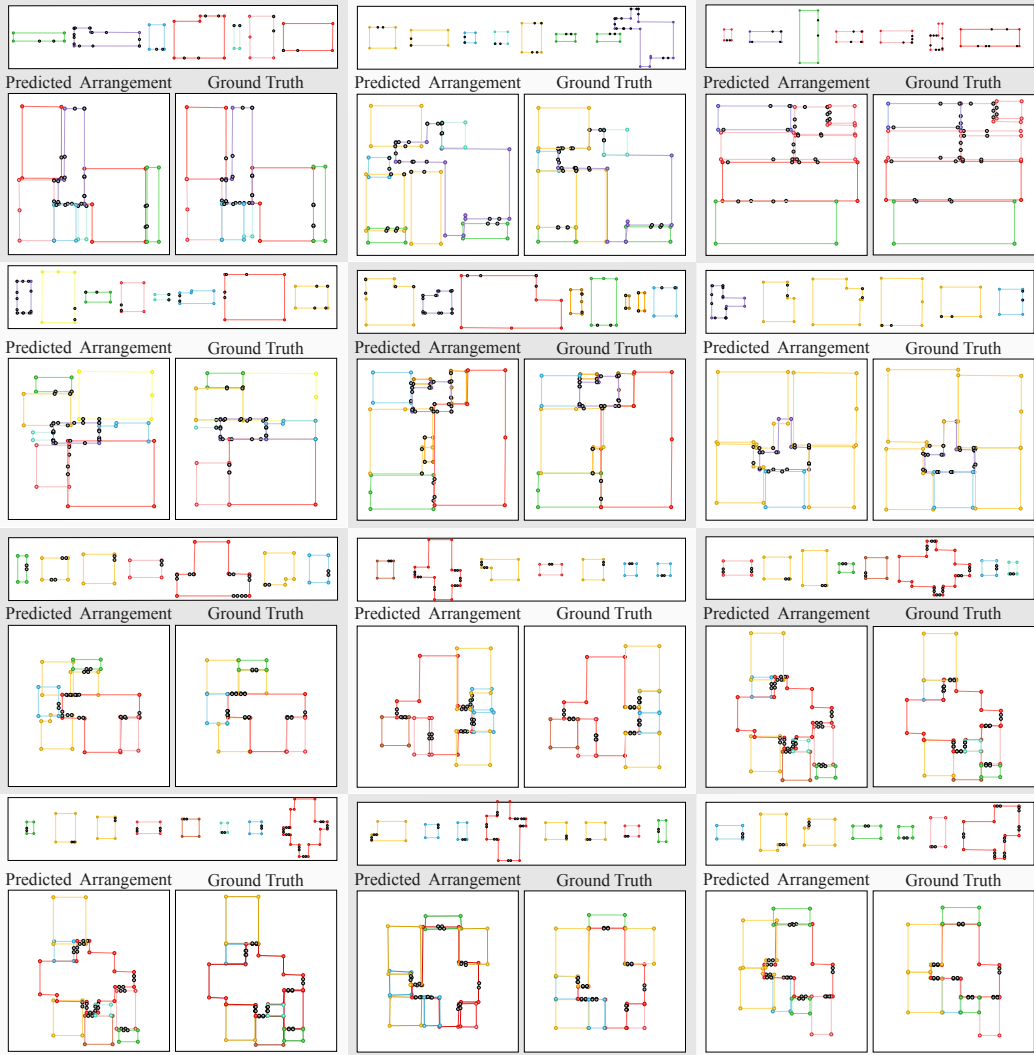


Figure 4: Qualitative evaluations of our method for Full MagicPlan dataset without GT rotations top two rows, and Full RPLAN dataset without GT rotations bottom two rows. We show edges and corners here to show overlaps and noisy annotations more clear.

117 **C.2.1 Pictorial Cross-cut Jigsaw Puzzle**

118 To enhance the integration of image information into our pictorial puzzle diffusion models, we  
 119 employed a two-step approach. Firstly, we pretrained an auto-encoder utilizing the puzzle pieces.  
 120 This auto-encoder served as the image embedder for our diffusion model, enabling the conversion of  
 121 each puzzle into a compact 128D feature vector.

122 The pretraining process involved training the model to downsample an input image of dimensions  
 123  $3 \times 256 \times 256$  to a compressed representation of size  $32 \times 2 \times 2$  within the encoder, and subsequently  
 124 reconstructing the original image size in the decoder. We employed the mean squared error (MSE)  
 125 loss function during training. However, to focus our model’s attention on learning the texture features,  
 126 given that the diffusion model already captured the geometry features, we applied the loss function  
 127 exclusively to the pixels within the puzzle piece.

128 By adopting this selective application of the loss function, we prioritize the acquisition of texture-  
 129 based details, as the geometric characteristics are already embedded within the diffusion model.

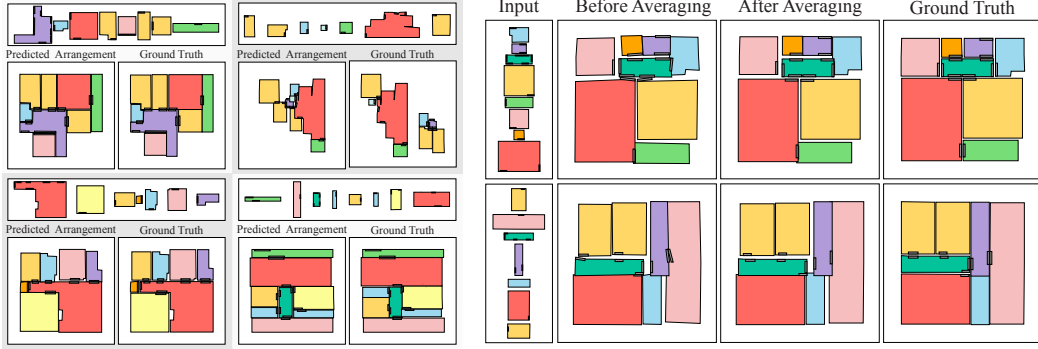


Figure 5: RLA arrangement results with Full MagicPlan dataset. On left two successful cases, on right two failed cases,. Our failures are often attributed to 1) Rare building architecture (top-right) and 2) Inherent ambiguity (bottom-right ), whose tasks are challenging even for humans.

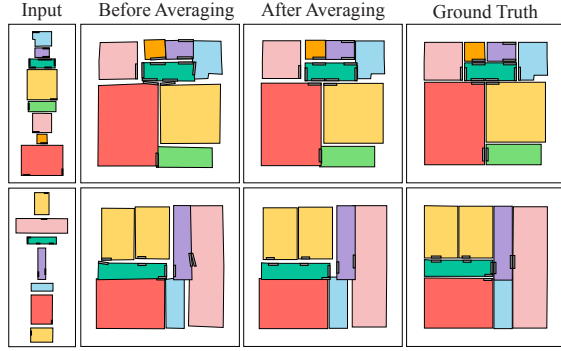


Figure 6: The final room arrangement before and after averaging. Our diffusion model estimates a room position/rotation at each room corner, which may not be consistent in a room. The final arrangement is obtained by taking the average position and rotation within each room.

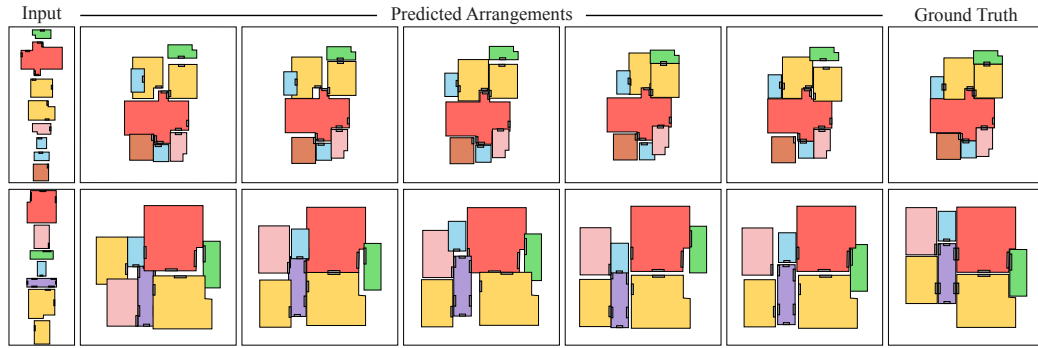


Figure 7: A diffusion model is stochastic and produces a different result every time. The middle rows show five different pose estimation results. The top (resp. bottom) is from Full RPLAN (resp. Full MagicPlan) dataset.

130 Quantitatively, we also evaluated our method on the full Cross-cut dataset to measure the effectiveness  
 131 of the pictorial information compared to apictorial scenario. We found that the model converges faster  
 132 when using pictorial information while it achieves slightly better overlap score of 0.9417 compared to  
 133 0.9398 in apictorial scenario. Figure 10 shows additional qualitative results of our method compared  
 134 to Harel *et al.* [3].

Table 5: Effects of the Missing or Duplicate pieces in puzzle solving problem.  $\checkmark$  indicates it if missing or duplicate piece were presented during test time. In training time we do not have duplicate or missing piece presented to show our model robustness to unseen noise during test.

		Cross-cut			Voronoi		
Missing	Duplicate	Overlap ( $\uparrow$ )	Precision ( $\uparrow$ )	Recall ( $\uparrow$ )	Overlap ( $\uparrow$ )	Precision ( $\uparrow$ )	Recall ( $\uparrow$ )
$\checkmark$	-	0.88	0.92	0.82	0.68	0.68	0.56
-	$\checkmark$	0.92	0.97	0.88	0.67	0.71	0.57
-	-	0.94	0.97	0.91	0.70	0.78	0.60

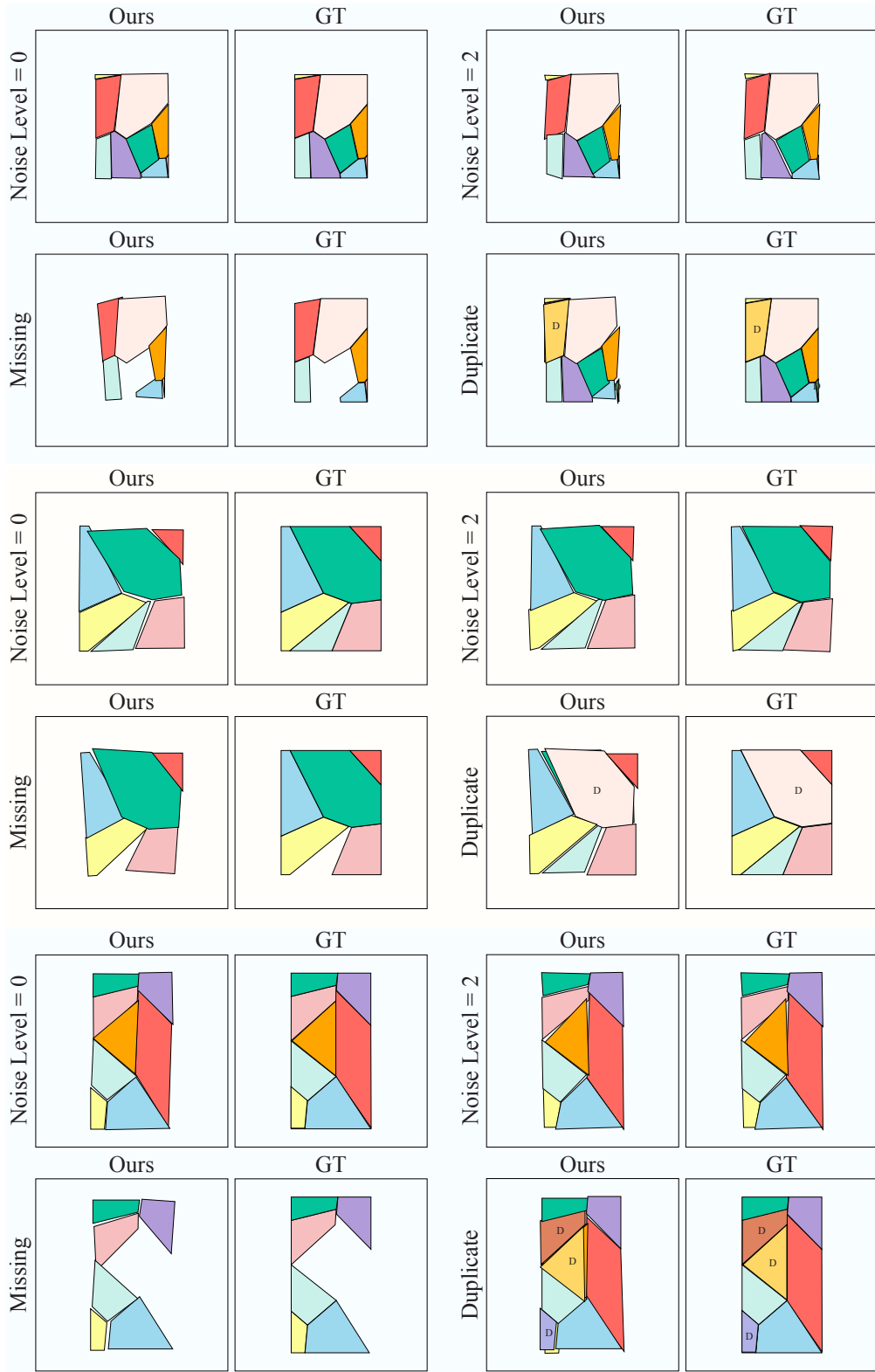


Figure 8: Additional qualitative results of Voronoi jigsaw puzzle are presented in four different setups: 1) No noise, 2) Noise level 2, 3) Missing piece, and 4) Duplicate piece (D indicates the duplicated pieces).

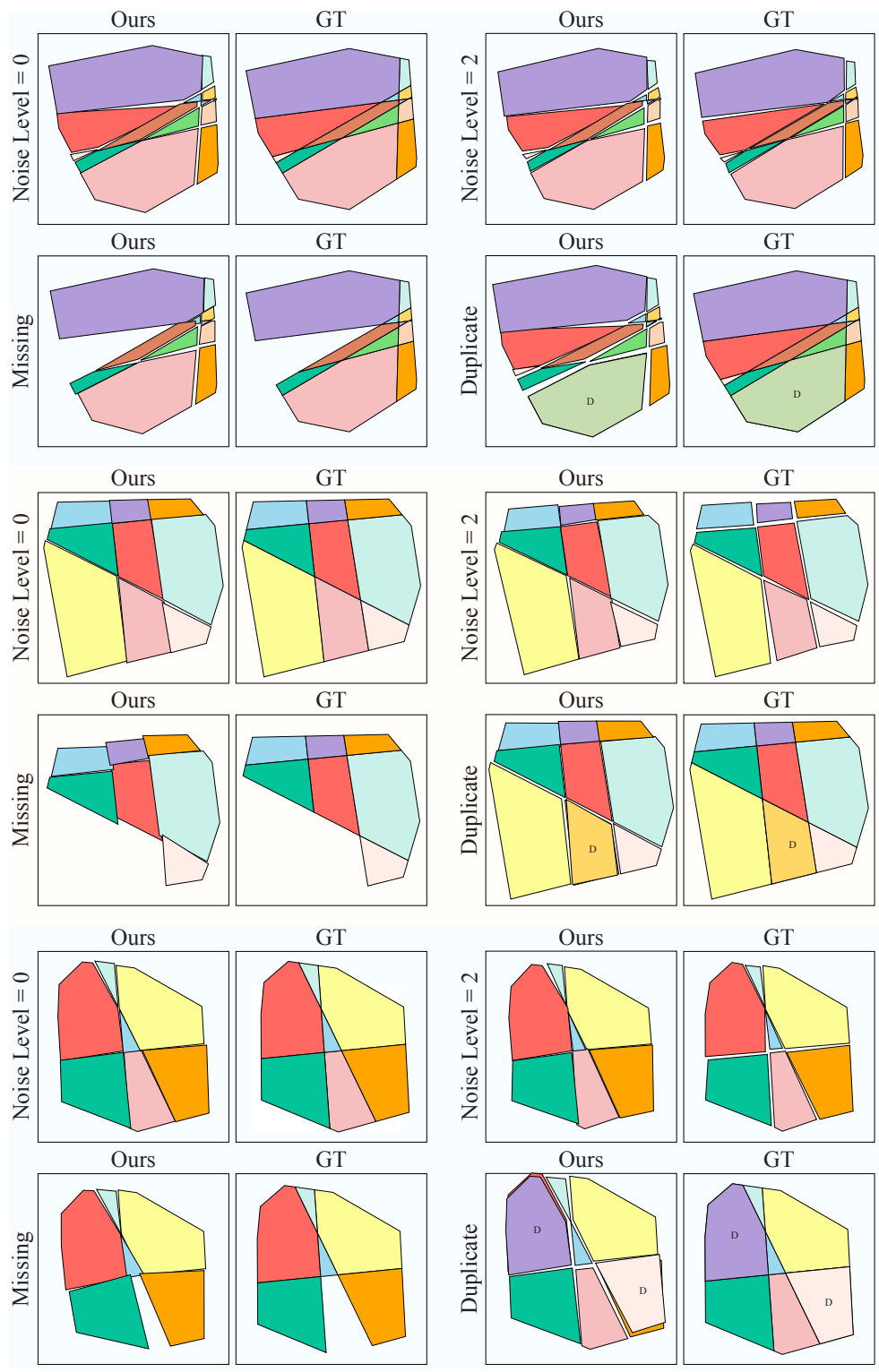


Figure 9: Additional qualitative results of Cross-cut jigsaw puzzle are presented in four different setups: 1) No noise, 2) Noise level 2, 3) Missing piece, and 4) Duplicate piece (D indicates the duplicated pieces).



Figure 10: Additional qualitative results of pictorial Cross-cut jigsaw puzzle compared to Harel *et al.* [3].

136 **References**

- 137 [1] Alexey Dosovitskiy, Lucas Beyer, Alexander Kolesnikov, Dirk Weissenborn, Xiaohua Zhai, Thomas  
138 Unterthiner, Mostafa Dehghani, Matthias Minderer, Georg Heigold, Sylvain Gelly, Jakob Uszkoreit, and  
139 Neil Houlsby. An image is worth 16x16 words: Transformers for image recognition at scale. *CoRR*,  
140 abs/2010.11929, 2020.
- 141 [2] Mohammad Amin Shabani, Weilian Song, Makoto Odamaki, Hirochika Fujiki, and Yasutaka Furukawa.  
142 Extreme structure from motion for indoor panoramas without visual overlaps. In *Proceedings of the*  
143 *IEEE/CVF International Conference on Computer Vision (ICCV)*, October 2021.
- 144 [3] Peleg Harel and Ohad Ben-Shahar. Crossing cuts polygonal puzzles: Models and solvers. In *Proceedings of*  
145 *the IEEE/CVF Conference on Computer Vision and Pattern Recognition*, pages 3084–3093, 2021.